Molecular Crystals and Liquid Crystals

ISSN: 1542-1406 (Print) 1563-5287 (Online) Journal homepage: http://www.tandfonline.com/loi/gmcl20

Preparation and Doping Effect of Surface Modified ZnS Nanoparticles on Liquid Crystal Nanocomposite System

Liping Wang, Fanguo Meng & Li Li

To cite this article: Liping Wang, Fanguo Meng & Li Li (2015) Preparation and Doping Effect of Surface Modified ZnS Nanoparticles on Liquid Crystal Nanocomposite System, Molecular Crystals and Liquid Crystals, 623:1, 104-112, DOI: 10.1080/15421406.2015.1017250

To link to this article: http://dx.doi.org/10.1080/15421406.2015.1017250

Published online: 21 Dec 2015.

Mol. Cryst. Liq. Cryst., Vol. 623: pp. 104–112, 2015

ISSN: 1542-1406 print/1563-5287 online
DOI: 10.1080/15421406.2015.1017250

Preparation and Doping Effect of Surface Modified ZnS Nanoparticles on Liquid Crystal Nanocomposite System

LIPING WANG,* FANGUO MENG AND LI LI

Department of Materials Physics and Chemistry, School of Materials Science and Engineering, University of Science and Technology Beijing, Beijing, P.R. China

A simple method was utilized to synthesize ZnS nanoparticles using mercaptoacetic acid as modifier in aqueous solution. XRD demonstrates that the ZnS nanoparticles have face-centered cubic structure. FT-IR spectroscopy shows that the stabilizer mercaptoacetic acid (MPA) is successfully modified on the surface of ZnS nanoparticles. A nanocomposite system was obtained by mixing the MPA modified ZnS nanoparticles with nematic liquid crystal 4'-pentyl-4-cyanobiphenyl (5CB). The doping effect on liquid crystal texture, liquid crystal transformation temperature, and ultraviolet absorption of the nanoparticles was investigated. The nanocomposite system remains the silky texture of the liquid crystal regardless of the addition of ZnS nanoparticles.

Keywords Liquid crystal; Nanocomposite; Surface modification; ZnS nanoparticles

Introduction

Nanocomposite materials have attracted increasing research interest in materials engineering due to their unique optical, electrical, and mechanical properties depending on the containing compositions [1]. Inorganic materials with special optical and electrical properties are good candidate compositions for the preparation of nanocomposites. Transition metal sulfide ZnS, a widely used II–VI group semiconductor with a wide band gap (3.68 eV) and an important luminescence material, has a great new technological application prospect in display, sensors, laser technology, biotechnology, and medicine based on its special chemical, physical, and electronic characteristics, and has been investigated intensively [2,3]. ZnS nanoparticles have been intensively studied in the past decades due to their unique size- and surface-related properties. Some properties of ZnS nanoparticles, such as luminescence, catalysis, and biocompatibility, can dramatically be changed by surface modification [4,5]. Furthermore, surface modified nanoparticles can be better applied to prepare nanocomposite materials and optimize their properties than unmodified ones.

Liquid crystals, the most widely used materials in display, have evoked exciting current research activities in liquid crystal-related nano-, micro-, and bio-technology other than in

*Address correspondence to Liping Wang, Department of Materials Physics and Chemistry, School of Materials Science and Engineering, University of Science and Technology Beijing, Beijing 100083, P.R. China. E-mail: lpwang@mater.ustb.edu.cn

Color versions of one or more of the figures in the article can be found online at www.tandfonline.com/gmcl.

displays or similar electro-optic devices [6]. Nanoparticle-doped liquid crystal nanocomposite system, which involves the integration of nanotechnology and liquid crystal display (LCD) technology, may provide new potential application in the nanocomposite field. The nanoparticle dopants used in liquid crystal nanocomposite system are mainly carbon nanotube [7,8], metal nanoparticles [9,10], metal and nonmetal oxide/sulfide nanoparticles [11–13], quantum dots [14], etc. The properties of the nanocomposite system significantly rely on the presence of nanoparticles and liquid crystal components and the interaction between them [15,16]. For instance, in the carbon nanotube doped composite system, carbon nanotubes can influence order of the surrounding liquid crystal domains [17] and physical properties [18]. For the liquid–crystal gel-dispersed quantum dot composite system containing core-shell CdSe/ZnS nanocrystals, reversible electrical modulation and switching of the photoluminescence intensity of quantum dots can be achieved [14]. However, surface modified ZnS nanoparticles have rarely been used in liquid crystal and investigated [19].

In the present work, mercaptoacetic acid (MPA) modified ZnS nanoparticles were prepared using a simple water phase synthetic method. Crystal and chemical structures of the modified ZnS nanoparticles were characterized by X-ray diffraction spectroscopy and Fourier transform-infrared spectroscopy. Moreover, a nanocomposite system of MPA-modified ZnS nanoparticles doped nematic liquid crystal 4′-pentyl-4-cyanobiphenyl (5CB) was prepared for the first time. The influence of ZnS nanoparticles on the texture, clearing temperature of the 5CB liquid crystal was studied, and the mutual influence on the ultraviolet (UV) absorption spectra between ZnS nanoparticles and the 5CB liquid crystal was investigated as well.

Experimental Details

Reagents and Instruments

Chemicals, zinc acetate [$Zn(CH_3COO)_2{\cdot}2H_2O$], mercaptoacetic acid ($HSCH_2COOH$), sodium sulfide, anhydrous ethanol, methylene chloride (CH_2Cl_2), and 5CB (4′-pentyl-4-cyanobiphenyl), were used as received.

A D/max-RB X-ray diffractometer (Rigaku Corp.) was used to characterize the phase structure of ZnS nanoparticles, using Cu Kα ($\lambda = 0.1542$ nm) irradiation. A 510P FT-IR infrared spectrometer (Nicolet Company USA) was used to characterize surface combination of the ZnS nanoparticles. For the composite system containing ZnS nanoparticles and 5CB liquid crystal, DSC-60 differential scanning calorimeter (Shimadzu Corp.) with a heating rate of $10^{\circ}C{\cdot}min^{-1}$ under nitrogen, BX51 polarizing optical microscope (POM) (Japan Olympus), and JASCO V570 UV-Vis-NIR spectrophotometer (Japan spectrophotometric instr.) were utilized to characterize clearing temperature, texture, and optical properties, respectively.

ZnS Nanoparticles Preparation and Composite with 5CB Liquid Crystal

MPA (138 μL) was added into a 5 mL of zinc acetate solution (0.2 $mol{\cdot}L^{-1}$), and then the solution was diluted to 50 mL, followed by magnetic stirring for 0.5 hr. Then, a 2 $mol{\cdot}L^{-1}$ solution of sodium hydroxide was added to adjust the pH value until it was 8, and the mixture was ventilated with nitrogen for 30 min. Under a condition of magnetic stirring and nitrogen ventilation, a 6.5 mL of sodium sulfide solution (0.2 $mol{\cdot}L^{-1}$) was carefully

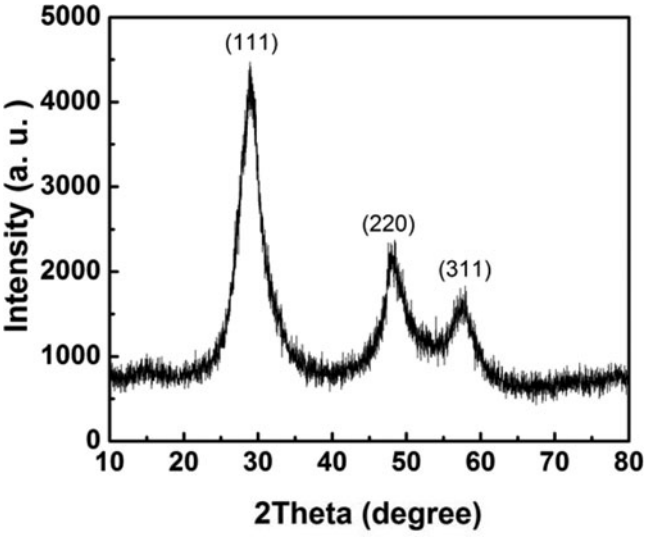

Figure 1. The XRD pattern of ZnS nanoparticles.

dropped into the solution, and kept stirring for 1 hr. After that, 100 mL of anhydrous ethanol was added to the emulsion to separate the product. After aging for 24 hr, the mixture was washed and centrifuged using deionized water and anhydrous alcohol twice, respectively. The precipitation was vacuum dried and a powder of MPA modified ZnS nanoparticles was obtained.

A well-dispersed composite mixture was obtained by mixing an appropriate amount of the prepared ZnS powder (0.001, 0.003, and 0.005 g, respectively) and 5CB liquid crystal (1.0 g), dissolved in a 1 mL solvent of methylene chloride, and sonicated for 30 min. The composite mixture was then placed in a vacuum oven to evaporate the solvent and finally filled into LC cells for further testing [20]. The substrate material, surface coating, and thickness of the cells were ITO glass, poly(vinyl alcohol) (PVA), and 25 μm, respectively.

Results and Discussion

XRD and IR Analysis of ZnS Nanoparticles

X-ray diffraction (XRD) pattern of the ZnS nanoparticles is shown in Fig. 1. All peaks can be well indexed to the zinc-blende phase (JCPDS No. 05-0566). The three diffraction peaks at 2θ values of 28.9°, 48.44°, and 57.92° correspond to the (110), (220), and (311) diffraction peaks, respectively. Diffraction peak broadening mainly due to minute particle size was observed, indicating the size is in nanometer range: Taking the (111) diffraction peak for calculation, the crystalline size is around 4 nm by the well-known Scherrer equation, $D = k\lambda/\beta cos\theta$. It is reported in the literature that doping effects of nanoparticles in nematic liquid crystals crucially depend on the size and shape of dopants [21].

Figure 2 shows the Fourier transform infrared (FT-IR) spectroscopy of MPA and a typical MPA modified ZnS nanoparticle sample. In Fig. 2(b), the peak at 3399 cm^{-1} is

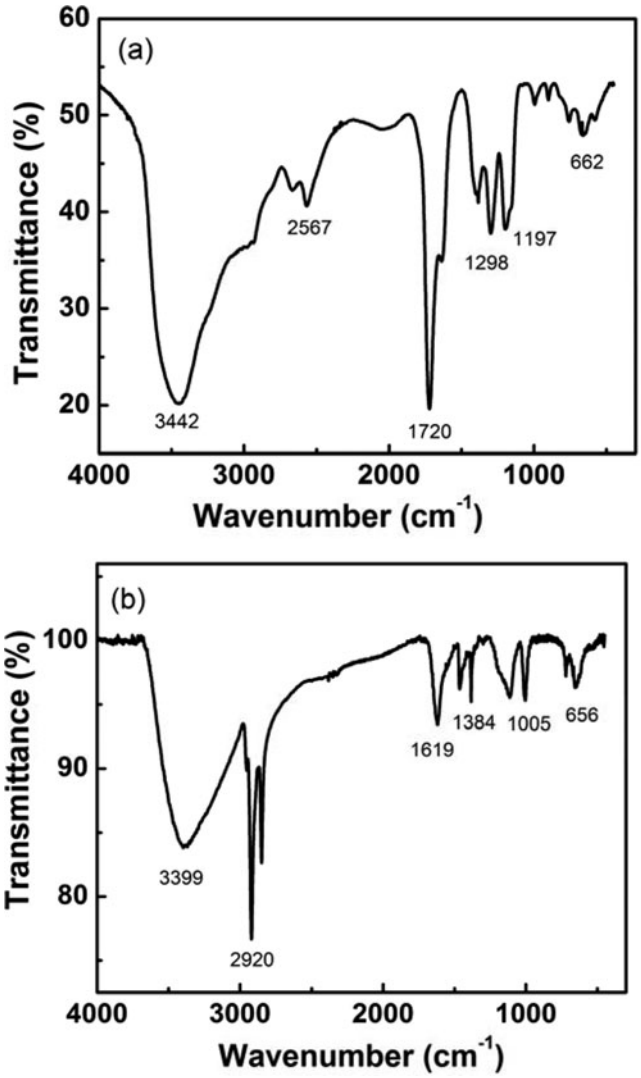

Figure 2. The Fourier transform-infrared (FT-IR) spectroscopy of mercaptoacetic acid (a) and a typical mercaptoacetic acid modified ZnS nanoparticle sample (b).

assigned to the $\nu_{\text{O-H}}$ vibration. Furthermore, the peak at 1619 cm^{-1} together with the peak at 3399 cm^{-1} suggests the presence of water, indicating the sample is not dried thoroughly. The peak at 2920 cm^{-1} is attributed to the stretching vibration of C—H bond in methylene group, ν_{CH2}, while the peak at 1384 cm^{-1} is attributed to the bending vibration of C—H bond in methyl group, δ_{CH3}. The weak peaks in the range of 600–700 cm^{-1} suggest the presence of C—S bond. However, the characteristic weak 2567 cm^{-1} peak, as shown in Fig. 2(a), which belongs to the stretching vibration of S—H bond in thiol group, $\nu_{\text{S-H}}$, does not exist. This indicates that the S—H bonds in MPA are destroyed during the preparation process. The result suggests that the MPA has been successfully modified on the surface of the ZnS nanoparticles.

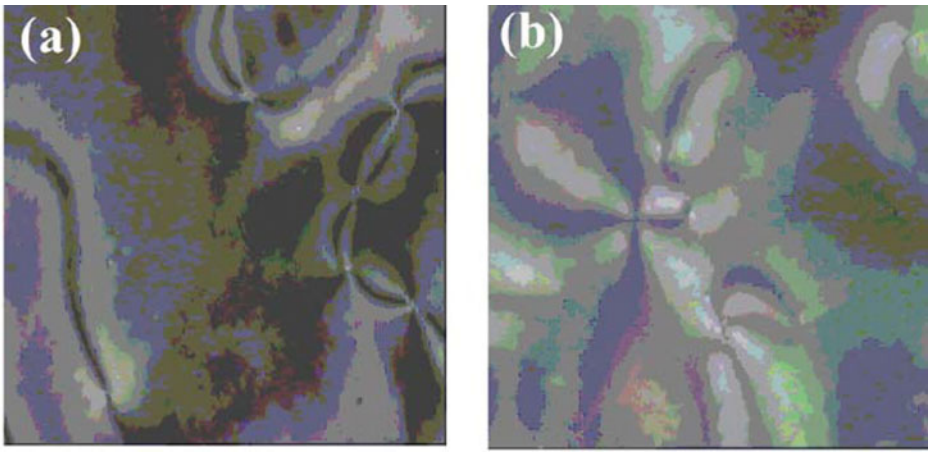

Figure 3. The texture of 5CB liquid crystal before (a) and after (b) doped with 0.3 wt% ZnS nanoparticles measured at room temperature.

Polarization and Clearing Temperature Analysis of the Liquid Crystal Composite System

Figure 3 shows the polarizing optical microscope (POM) of pure 5CB and the ZnS doped liquid crystal composite system. Compared with the POM image of 5CB liquid crystal (Fig. 3a) and the one (Fig. 3b) of 5CB doped with 0.3 wt% ZnS nanoparticles, both of the liquid crystal systems have Schlieren-texture. The result suggests that the addition of the ZnS nanoparticles does not have much impact on the 5CB liquid crystal texture, and the textures maintain the nematic order. The present result is in consistent with the one reported for the octadecylamine covered CdSe/ZnS core/shell quantum dots [22]. The rod-like liquid molecules adjacent to the nanoparticles with covering ligands may orient in a radial arrangement. This may cause a slight mismatch between the director field at the surface of nanoparticles and the nematic director. As a result, the observed Schlieren texture is trivial. However, other factors, such as film thickness, capping agent, and the type, size, and amount of nanoparticles, should be taken into account. Investigation reported in literature [23] for liquid crystal system doped with hexadecylamine-capped CdSe and thioglycolic acid-capped CdTe quantum dots shows significant alignment in POM images. Due to the similarity of the above mentioned system and the one studied herein, it can be deduced that in rubbed test cells with a larger thickness and higher doping concentration of nanoparticles the Schlieren texture could be seen more obviously.

Figure 4 shows the clearing temperature of 5CB liquid crystal doped with the ZnS nanoparticles. The clearing temperature of the liquid crystal is substantially reduced, which is lower than that of the un-doped 5CB, and the largest clearing temperature decline is nearly 10°C for the sample of 5CB doped with 0.1wt% ZnS nanoparticles. Moreover, as the doping concentration increases, the clearing temperature for the ZnS nanoparticles doped 5CB liquid crystal decreases, which might be due to the interaction between surface modifier and adjacent 5CB molecules. This observation is in agreement with the theoretical research reported in literature [24]. This observation is also similar to the one reported by T. Hegmann et al. [25], which systematically investigated a system of liquid crystal silane-functionalized gold nanoparticles (AuNPs) nanocomposites and states that higher concentrations of AuNPs even led to a slight decrease in the phase-transition temperatures.

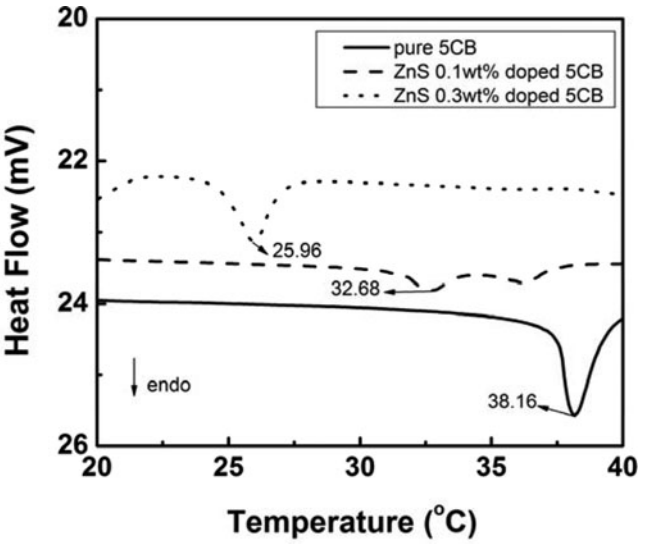

Figure 4. Clearing temperature of the 5CB liquid crystal doped with the ZnS nanoparticles recorded on DSC with cooling.

Generally speaking, the change of clearing temperature is critical in application, especially for the thermotropic liquid crystal. The reduction in clearing temperature suggests that the doped 5CB liquid crystal composite system can be used in such applications that require narrow temperature range.

Ultraviolet Absorption Spectra Analysis of the Composite System

Figure 5 shows the ultraviolet (UV) absorption spectra of the ZnS nanoparticles. The measurement was carried out at room temperature. There is a UV absorption peak at

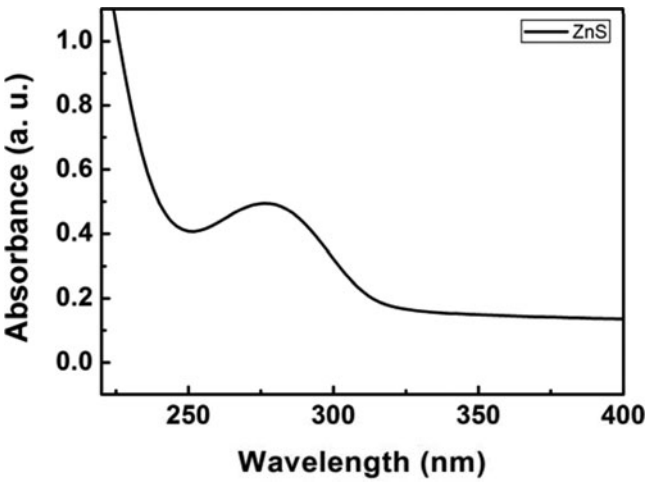

Figure 5. UV absorption spectrum of ZnS nanoparticles.

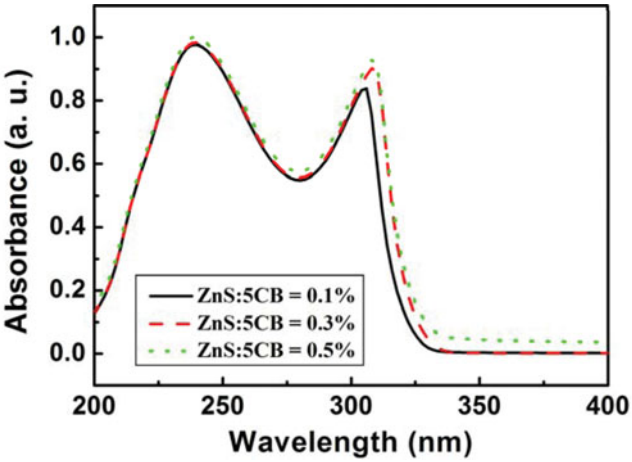

Figure 6. UV absorption spectra of ZnS nanoparticles doped 5CB liquid crystal.

around 279 nm for the ZnS nanoparticles in Fig. 5. While for the pure 5CB liquid crystal, its UV absorption spectra can be found in literature [26,27]. There are two major absorption bands (designated as λ_1 and λ_2, $\lambda_1 < \lambda_2$) in the 190–400 nm region, which result from the π–π^* electronic transition of the two benzene rings in 5CB liquid crystal molecules. One band appears in a wavelength range of 190–210 nm, and the other appears in 250–310 nm. The absorption intensity for each band is very strong. In addition, our experiment showed that the absorption ranging from 250 to 310 nm would be saturated if the concentration was high.

Figure 6 shows the UV absorption spectra of ZnS nanoparticles doped 5CB liquid crystal for three different doping concentrations (0.1 wt%, 0.3 wt%, 0.5 wt%), which were measured at room temperature. For the composite of ZnS nanoparticles doped 5CB, the UV absorption peak of the ZnS nanoparticles around 279 nm does not appear. However, the absorption of ZnS nanoparticles should exist and construct with that of 5CB liquid crystal, resulting in the UV spectra shown in Fig. 6, which is different from the UV spectra of 5CB [26,27]. This implies that the addition of 5CB liquid crystal almost may not affect the UV absorption spectrum of ZnS nanoparticles. As shown in Fig. 6, the first absorption peaks on the left are almost the same for the samples of a certain amount 5CB liquid crystal molecules doped with various ZnS nanoparticles. While for the second absorption peaks, as the doping concentration of ZnS nanoparticles increases, there is a slight growth of the absorption peak. This result may be attributed to the changing in spatial arrangement of the 5CB liquid crystal molecules due to the addition of nanoparticles [28]. The orientational order of the 5CB liquid crystal molecules is decreased by the addition of ZnS nanoparticles in some adjacent regions [29]. Although the nanoparticles are about the length of several liquid crystal molecules in size, they tend to aggregate to form larger particles due to their instability. Therefore, the presence of larger nanoparticles may have impact on liquid crystal molecule ordering, causing distortion in some regions, which is radial sorting rather than parallel in the regions around the nanoparticles. One the other hand, for the second absorption peak of liquid crystal molecules, the reason for the intensity enhancement and the red-shift is not very clear and further investigation may be required. We speculate that the change in UV absorption of 5CB might result from some influence of the MPA modified ZnS nanoparticles on the benzene ring bonded to the –CN group because some interactions,

such as hydrogen bonding, may form between the –OH group and the nitrogen atom in –CN group. Moreover, as the doping content of the nanoparticles increases, the content of MPA increases and this impact on the structure may increase gradually. As a result, there is a slight intensity increase and a red-shift in wavelength.

Conclusion

MPA modified ZnS nanoparticles with zinc blende structure were synthesized by means of a simple aqueous synthesis method. FT-IR results show that the stabilizer MPA is successfully modified on the surface of ZnS nanoparticles. The composites of the prepared nanoparticles and liquid crystal dissolve completely in methylene chloride, which determines the influence of both components. The nanoparticles do not have observable effect on the silky texture of the liquid crystal, while they do have effect on the liquid crystal clearing temperature to a certain extent. With increasing doping concentration of ZnS nanoparticles, the clearing temperature of the liquid crystal decreases. In addition, the doping of MPA modified nanoparticles has definite impact on the UV absorption peak of the liquid crystal.

Funding

Financial support from the National Natural Science Foundation of China (Grant no. 21073012, and 20773012) is greatly acknowledged.

References

[1] Beecroft, L. L., & Ober, C. K. (1997). *Chem. Mater.*, *9*, 1302.
[2] Mehta, S. K., Kumar, S., & Gradzielski, M. (2011). *J. Colloid Interf. Sci.*, *360*, 497.
[3] Wang, Q. B., Xu, Y., Zhao, X. H., Chang, Y., Liu, Y., Jiang, L. J., Sharma, J., Seo, D.-K., & Yan, H. (2007). *J. Am. Chem. Soc.*, *129*, 6380.
[4] Kulkarni, S. K., Winkler, U., Deshmukh, N., Borse, P. H., Fink, R., & Umbach, E. (2001). *Appl. Surf. Sci.*, *169–170*, 438.
[5] Hartono, D., Qin, W. J., Yang, K.-L., & Yung, L.-Y. L. (2009). *Biomaterials*, *30*, 843.
[6] Lagerwall, J. P. F., & Scalia, G. (2012). *Curr. Appl. Phys.*, *12*, 1387.
[7] Lee, W., Wang, C.-Y., & Shih, Y.-C. (2004). *Appl. Phys. Lett.*, *85*, 513.
[8] Kamanina, N. V., Reshak, A. H., Vasilyev, P. Va., Vangonen, A. I., Studeonov, V. I., Usanov, Y. E., Ebothe, J., Gondek, E., Wójcik, W., & Danel, A. (2009). *Physica E*, *41*, 391.
[9] Reznikov, Y., Buchnev, O., Tereshchenko, O., Reshetnyak, V., Glushchenko, A., & West, J. (2003). *Appl. Phys. Lett.*, *82*, 1917.
[10] Shiraishi, Y., Toshima, N., Maeda, K., Yoshikawa, H., Xu, J., & Kobayashi, S. (2002). *Appl. Phys. Lett.*, *81*, 2845.
[11] Dolgov, L. O., & Yaroshchuk, O. V. (2004). *Colloid Polym. Sci.*, *282*, 1403.
[12] Mercuri, F., Ghosh, A. K., & Marinelli, M. (1999). *Phys. Rev. E*, *60*, 6309.
[13] Lorenz, A., Zimmermann, N., Kumar, S., Evans, D.R., Cook, G., & Kitzerow, H.-S. (2012). *Phys. Rev. E*, *86*, 051704.
[14] Tong, X., & Zhao, Y. (2007). *J. Am. Chem. Soc.*, *129*, 6372.
[15] Gupta, M., Satpathy, I., Roy, A., & Pratibha, R. (2010). *J. Colloid Interf. Sci.*, *352*, 292.
[16] Duran, H., Gazdecki, B., Yamashita, A., & Kyu, T. (2005). *Liq. Cryst.*, *32*, 815.
[17] Mrozek, R. A., Kim, B.-S., Holmberg, V. C., & Taton, T. A. (2003). *Nano Lett.*, *3*, 1665.
[18] Kim, J. Y., Kim, D. K., & Kim, S. H. (2009). *Eur. Polym. J.*, *45*, 316.
[19] Wang, L., Meng, F., Sun, Y., & Yang, H. (2013). *Composite B*, *45*, 780.
[20] Lorenz, A., Agra-Kooijman, D., Zimmermann, N., Kitzerow, H.-S., Evans, D., & Kumar, S. (2013). *Phys. Rev. E*, *88*, 062505.

[21] Qi, H., & Hegmann, T. (2011). *Liq. Cryst. Today*, *20*, 102.
[22] Rodarte, A.L., Pandolfi, R.J., Ghosh, S., & Hirst, L.S. (2013). *J. Mater. Chem. C*, *1*, 5527.
[23] Kinkead, B., Hegmann, T. (2010). *J. Mater. Chem.*, *20*, 448.
[24] Gorkunov, M. V., & Osipov, M. A. (2011). *Soft Matter*, *7*, 4348.
[25] Mirzaei, J., Urbanski, M., Kitzerow, H.-S., & Hegmann, T. (2014). *Chem. Phys. Chem.*, *15*, 1381.
[26] Wu, S.-T., Ramos, E., & Finkenzeller, U. (1990). *J. Appl. Phys.*, *68*, 78.
[27] Wu, S.-T. (1998). *J. Appl. Phys.*, *84*, 4462.
[28] Voloschenko, D., Pishnyak, O.P., Shiyanovskii, S.V., & Lavrentovich, O.D. (2002). *Phys. Rev. E*, *65*, 060701.
[29] Lorenz, A., Zimmermann, N., Kumar, S., Evans, D. R., Cook, G., Fernández Martínez, M., & Kitzerow, H.-S. (2013). *J. Phys. Chem. B*, *117*, 937.